Comput. Mech. (2006) 39: 25–40
DOI 10.1007/s00466-005-0006-9

ORIGINAL PAPER

L. Marin

Numerical boundary identification for Helmholtz-type equations

Received: 28 May 2005 / Accepted: 5 July 2005 / Published online: 26 October 2005

Abstract We study the identification of an unknown portion of the boundary of a two-dimensional domain occupied by a material satisfying Helmholtz-type equations from additional Cauchy data on the remaining known portion of the boundary. This inverse geometric problem is approached using the boundary element method (BEM) in conjunction with the Tikhonov first-order regularization procedure, whilst the choice of the regularization parameter is based on the L-curve criterion. The numerical results obtained show that the proposed method produces a convergent and stable solution.

Keywords Inverse problem · Boundary identification · Helmholtz-type equations · Boundary element method (BEM) · L-curve

1 Introduction

A direct problem in the mathematical modelling of physical systems is to determine the response of a system when the governing partial differential equations, the geometry of the domain of interest, the complete boundary and initial conditions, the material properties and the external sources acting in the domain are given, see e.g., Kubo [1]. When one or more of these conditions for solving the direct problem are partially or entirely unknown then an inverse problem may be formulated to determine the unknowns from specified or measured system responses. It should be noted that most of the inverse problems are ill-posed and hence they are more difficult to solve than direct problems. It is well known that inverse problems are in general unstable, see e.g., Hadamard [2], in the sense that small measurement errors in the input data may amplify significantly the errors in the solution.

In recent years, inverse problems have been extensively treated in several branches of science and an overview of the developments in engineering is available in Kubo [1]. The most common approach is to determine the optimal estimates of the model parameters by minimising a selected measure-of-fit between the responses of the system and the model. An important class of inverse problems in engineering consists of the inverse geometrical problems which can be divided into the following subclasses: shape and design optimisation [3–7], identification of defects, e.g. cracks, cavities or inclusions, [8–14] and identification of an unknown boundary [15–24].

With respect to the later subclass of inverse geometrical problems, it should be noted that most of the theoretical and numerical studies are devoted to the Laplace equation. Aparicio and Pidcock [15] have studied the problem of determining a part of the boundary of a domain, where a potential satisfies the Laplace equation, and have proposed two methods to solve this problem, provided that the potential is monotonic along the unknown boundary. The stability of determining a portion of the boundary, which encloses a two-dimensional bounded domain where the Laplace equation is satisfied, from Cauchy data has been undertaken by Beretta and Vessela [16]. Various conditional stability estimates for this problem, according to a priori assumptions on the regularity of the unknown sub-boundaries, have been given by Bukhgeim et al. [17]. Hsieh and Kassab [18] have proposed a general numerical method in order to determine an unknown boundary for heat conduction problems which is independent of the type of condition imposed at the unknown boundary. Huang and Chao [19] have studied a steady-state shape identification problem by using both the Levenberg-Marquardt method and the conjugate gradient method. Their work has been extended by Huang and Tsai [20] to a transient inverse geometrical problem in identifying the irregular boundary configurations from external measurements using the boundary element method (BEM). Based on the idea of radial basis interpolation for Hermite-Birkhoff data and the shape

L. Marin
School of Earth and Environment, Environment Centre,
University of Leeds, Leeds LS2 9JT, UK

L. Marin (✉)
School of Mechanical, Materials and Manufacturing Engineering,
The University of Nottingham, University Park,
Nottingham NG7 2RD, UK
Tel.: +44-(0)115-846 7683
Fax: +44-(0)115-951 3800
E-mail: liviu.marin@nottingham.ac.uk

invariability of harmonic function space, a non-destructive method has been proposed by Hon and Wu [21] in order to determine an unknown boundary of a domain from given values of a harmonic function and its derivatives on the remaining part of the boundary. Park and Ku [22] have considered the inverse problem of identifying the boundary shape of a domain from boundary temperature measurements, where the temperature is dominated by natural convection. Lesnic et al. [23] have studied the boundary determination in potential corrosion damage from Cauchy data available on the known boundary of the solution domain and, recently, their method has been extended to linear elastic materials by Marin and Lesnic [24].

Helmholtz-type equations arise naturally in many physical applications related to wave propagation, vibration phenomena and heat transfer. These equations are often used to describe the vibration of a structure [25], the acoustic cavity problem [26], the radiation wave [27], the scattering of a wave [28] and the heat conduction in fins [29]. To our knowledge, the identification of an unknown portion of the boundary of a two-dimensional domain, where Helmholtz-type equations are satisfied, from additional Cauchy data on the remaining portion of the boundary has not, as yet, been investigated. This inverse geometrical problem is approached in a similar manner to that by Lesnic et al. [23] and Marin and Lesnic [24]. The BEM is employed in conjunction with the Tikhonov first-order regularization procedure, with the choice of the regularization parameter based on the L-curve criterion [30], although one may use the Morozov discrepancy principle [31] or the generalised cross-validation principle [32].

2 Mathematical formulation

Referring to heat transfer for the sake of the physical explanation, we assume that the temperature field $T(\underline{x})$ satisfies the Helmholtz-type equation in an open bounded domain $\Omega \subset \mathbb{R}^2$, namely

$$\mathcal{L}T(\underline{x}) \equiv \left(\Delta \pm k^2\right) T(\underline{x}) = 0, \quad \underline{x} \in \Omega, \tag{1}$$

where $k > 0$, while the plus and minus signs correspond to the Helmholtz and the modified Helmholtz equations, respectively. Additionally, we assume that the boundary $\Gamma \equiv \partial\Omega$ is smooth in the sense of Liapunov such that Green's formula is applicable [33].

The general equation describing the temperature distribution along an isolated fin for steady state two-dimensional heat transfer is obtained by completing a heat balance over an incremental surface element, $\mathrm{d}\underline{z} = (z_1 - \mathrm{d}z_1/2, z_1 + \mathrm{d}z_1/2) \times (z_2 - \mathrm{d}z_2/2, z_2 + \mathrm{d}z_2/2)$, at some point, $\underline{z} = (z_1, z_2)$ within the fin surface, see e.g., Kraus et al. [29]. The heat balance over the increment, $\mathrm{d}\underline{z}$, for steady state heat flow is given by

$$\begin{aligned}&\left(\dot{Q}_f(z_1 - \mathrm{d}z_1/2, z_2) - \dot{Q}_f(z_1 + \mathrm{d}z_1, z_2/2)\right)\mathrm{d}z_2\\ &+ \left(\dot{Q}_f(z_1, z_2 - \mathrm{d}z_2/2) - \dot{Q}_f(z_1, z_2 + \mathrm{d}z_2/2)\right)\mathrm{d}z_1\\ &- \dot{Q}_c(z_1, z_2) = 0,\end{aligned} \tag{2}$$

where $\dot{Q}_f(z_1, z_2)$ is the conductive heat flow at $\underline{z} = (z_1, z_2)$ and $\dot{Q}_c(z_1, z_2)$ is the heat lost from the incremental surface of the fin. From the Postulation of Fourier, we have

$$\dot{Q}_f(z_1, z_2) = -\lambda_f A_f \nabla\theta_f(z_1, z_2), \tag{3}$$

where λ_f is the thermal conductivity of the fin and A_f is the cross-sectional area of the fin, and by using a Taylor series expansion around $\underline{z} = (z_1, z_2)$ and neglecting terms after the first-order derivatives we obtain

$$\begin{aligned}&\left(\dot{Q}_f(z_1 - \mathrm{d}z_1/2, z_2) - \dot{Q}_f(z_1 + \mathrm{d}z_1/2, z_2)\right)\mathrm{d}z_2\\ &+ \left(\dot{Q}_f(z_1, z_2 - \mathrm{d}z_2/2) - \dot{Q}_f(z_1, z_2 + \mathrm{d}z_2/2)\right)\mathrm{d}z_1\\ &= \nabla \cdot \left(\lambda_f A_f \nabla\theta_f(z_1, z_2)\right)\, \mathrm{d}z_1\mathrm{d}z_2.\end{aligned} \tag{4}$$

The heat lost from the surface of the incremental fin is assumed to be by convection and, by Newton's law of cooling, this is given by

$$\dot{Q}_c(z_1, z_2) = hA'_f \left(\theta_f(z_1, z_2) - \theta_\infty\right)\mathrm{d}z_1\mathrm{d}z_2, \tag{5}$$

where h is the surface heat transfer coefficient, A'_f is the surface area of the fin per unit length and θ_∞ is the temperature of the surrounding medium.

Substitution of Eq. (4) and (5) into the heat balance Eq. (2) provides the following second-order partial differential equation:

$$\nabla \cdot \left(\lambda_f A_f \nabla\theta_f(\underline{z})\right) - hA'_f \left(\theta_f(\underline{z}) - \theta_\infty\right) = 0. \tag{6}$$

The following assumptions are invoked in order to obtain the general fin equation:

(i) The thermal conductivity of the fin, λ_f, is invariant;
(ii) The surface heat transfer coefficient, h, is uniform along the fin;
(iii) The temperature of the surrounding medium, θ_∞, is constant.

Additionally, if we assume that the cross-sectional area of the fin is constant (i.e., the fin thickness, $2\delta_f$, is invariant) then the fin equation (6) recasts as

$$\Delta\theta_f(\underline{z}) - \frac{h}{\lambda_f \delta_f}\left(\theta_f(\underline{z}) - \theta_\infty\right) = 0. \tag{7}$$

On introducing the following dimensionless variables:

$$\begin{aligned}&x_j = z_j/\delta_f, \quad j = 1, 2,\\ &T(\underline{x}) = \left(\theta_f(\underline{z}) - \theta_\infty\right) / \left(\theta_b - \theta_\infty\right),\end{aligned} \tag{8}$$

where θ_b is the fin base temperature ($\theta_b \neq \theta_\infty$), then the non-dimensional temperature distribution along an isolated fin of constant cross-sectional area for steady state two-dimensional heat transfer is described by the Helmholtz-type equation (1) with $\mathcal{L} = \Delta - k^2$ and $k = \sqrt{h/\left(\lambda_f \delta_f\right)}$.

We now let $\underline{\nu}(\underline{x})$ be the outward normal vector at the boundary Γ and $\Phi(\underline{x}) \equiv (\partial T/\partial\underline{\nu})(\underline{x})$ be the flux at a point $\underline{x} \in \Gamma$. In the direct problem formulation, the knowledge of the constant k, the location, shape and size of the entire

boundary Γ, and the temperature and/or flux on the boundary Γ gives the corresponding Neumann, Dirichlet, or mixed boundary problems which enable one to determine the temperature $T(\underline{x})$ in the domain Ω. A different and more interesting inverse situation occurs when a part of the boundary Γ is unknown and some additional information is supplied on the remaining part of the boundary. More specifically, we analyse the following problem:

Find the boundary $\Gamma_2 \subset \Gamma$, $\Gamma_2 \neq \emptyset$, such that the temperature $T(\underline{x})$ satisfies the Helmholtz-type equation (1), either Dirichlet or Neumann boundary conditions are given on Γ_2 and the temperature and the flux, i.e. Cauchy data, are known on the remaining part $\Gamma_1 = \Gamma \setminus \Gamma_2$ of the boundary, namely

$$T(\underline{x}) = \widetilde{T}(\underline{x}) \quad \text{and} \quad \Phi(\underline{x}) = \widetilde{\Phi}(\underline{x}), \quad \underline{x} \in \Gamma_1, \tag{9}$$

$$T(\underline{x}) = \widetilde{T}(\underline{x}) \quad \text{or} \quad \Phi(\underline{x}) = \widetilde{\Phi}(\underline{x}), \quad \underline{x} \in \Gamma_2. \tag{10}$$

3 Boundary element method

Let E_{H} and E_{MH} be the fundamental solutions of the Helmholtz and the modified Helmholtz equations, respectively, which in two-dimensions are given by, see e.g., Chen and Zhou [34],

$$\begin{aligned} E_{\mathrm{H}}(\underline{x}, \underline{y}) &= \frac{\mathrm{i}}{4} H_0^{(1)}\left(k\,|\underline{y} - \underline{x}|\right), \\ E_{\mathrm{MH}}(\underline{x}, \underline{y}) &= \frac{1}{2\pi} K_0\left(k\,|\underline{y} - \underline{x}|\right), \end{aligned} \tag{11}$$

where $H_0^{(1)}$ is the Hankel function of the first kind of order zero, K_0 is the modified Bessel function of the second kind of order zero and $\underline{x}, \underline{y} \in \mathbb{R}^2$. The Helmholtz-type Eq. (1) can also be formulated in integral form [34] as

$$\begin{aligned} &c(\underline{x}) T(\underline{x}) + \int_{\Gamma} \frac{\partial E(\underline{x}, \underline{y})}{\partial \underline{v}(\underline{y})} T(\underline{y})\, \mathrm{d}\Gamma(\underline{y}) \\ &= \int_{\Gamma} E(\underline{x}, \underline{y}) \Phi(\underline{y})\, \mathrm{d}\Gamma(\underline{y}), \underline{x} \in \overline{\Omega} \equiv \Omega \cup \Gamma, \end{aligned} \tag{12}$$

where the first integral is taken in the sense of the Cauchy principal value, $c(\underline{x}) = 1$ for $\underline{x} \in \Omega$, $c(\underline{x}) = 1/2$ for $\underline{x} \in \Gamma$ (smooth) and $E = E_{\mathrm{H}}$ or $E = E_{\mathrm{MH}}$.

Following a classical BEM, see Marin et al. [35,36], the boundary Γ of the solution domain Ω is discretised in an anti-clockwise direction into N constant boundary elements $\Gamma^{(n)} = \left[\underline{y}^{(n-1)}, \underline{y}^{(n)}\right]$, $n = 1, \ldots, N$, having the mid-points/collocation points $\underline{x}^{(n)} = \left(x_1^{(n)}, x_2^{(n)}\right)$, where $\underline{x}^{(n)} = \left(\underline{y}^{(n-1)} + \underline{y}^{(n)}\right)/2$, $n = 1, \ldots, N$, and $\underline{y}^{(0)} \equiv \underline{y}^{(N)}$. On applying the constant BEM approximation in which the temperature and the flux are assumed constant over each boundary element $\Gamma^{(n)}$, we obtain

$$\begin{aligned} T(\underline{y}) &= T(\underline{x}^{(n)}) \equiv T_n, \\ \Phi(\underline{y}) &= \Phi(\underline{x}^{(n)}) \equiv \Phi_n, \\ &\underline{y} \in \Gamma^{(n)}, \quad n = 1, \ldots, N. \end{aligned} \tag{13}$$

If the boundaries Γ_1 and Γ_2 are discretised into N_1 and N_2 boundary elements, respectively, such that $N = N_1 + N_2$, then it should be noted that the unknown boundary Γ_2 is completely determined by the vector $\underline{Y} = \left(\underline{y}^{(N_1+1)}, \ldots, \underline{y}^{(N-1)}\right)^T \in \mathbb{R}^{2(N_2-1)}$, i.e., $\Gamma_2 = \Gamma_2\left(\underline{Y}\right)$. Thus relation (12) recasts as

$$\begin{aligned} &c(\underline{x}) T(\underline{x}) + \sum_{n=1}^{N} A_n\left(\underline{x}, \underline{Y}\right) T_n \\ &= \sum_{n=1}^{N} B_n\left(\underline{x}, \underline{Y}\right) \Phi_n, \quad \underline{x} \in \overline{\Omega}, \end{aligned} \tag{14}$$

where

$$\begin{aligned} A_n\left(\underline{x}, \underline{Y}\right) &= \int_{\Gamma_n} \frac{\partial E(\underline{x}, \underline{y})}{\partial \underline{v}(\underline{y})}\, \mathrm{d}\Gamma(\underline{y}), \\ B_n\left(\underline{x}, \underline{Y}\right) &= \int_{\Gamma_n} E(\underline{x}, \underline{y})\, \mathrm{d}\Gamma(\underline{y}), \quad \underline{x} \in \overline{\Omega}. \end{aligned} \tag{15}$$

Collocating equation (14) at each boundary node $\underline{x}^{(m)}$, $m = 1, \ldots, N$, we arrive at the system of equations

$$\sum_{n=1}^{N} \left\{A_{mn}\left(\underline{Y}\right) T_n - B_{mn}\left(\underline{Y}\right) \Phi_n\right\} = 0, \quad m = 1, \ldots, N, \tag{16}$$

where $A_{mn}\left(\underline{Y}\right)$ and $B_{mn}\left(\underline{Y}\right)$ are given by

$$\begin{aligned} A_{mn}\left(\underline{Y}\right) &= c(\underline{x}^{(m)}) + A_n\left(\underline{x}^{(m)}, \underline{Y}\right), \\ B_{mn}\left(\underline{Y}\right) &= B_n\left(\underline{x}^{(m)}, \underline{Y}\right), \quad m, n = 1, \ldots, N. \end{aligned} \tag{17}$$

Details regarding the computation of the integration constants for constant boundary elements associated with two-dimensional Helmholtz-type equations are given in Sect. *A*.

4 Description of the algorithm

In the sequel, we focus on the inverse geometric problem given by Eqs. (1), (9) and (10_1), with the mention that the problem given by Eqs. (1), (9) and (10_2) can be treated in a similar manner. If we consider the discretised BEM system (16) recast as the solution of a direct problem with boundary conditions (9_2) and (10_1), namely

$$\begin{aligned} &\sum_{n=1}^{N_1} A_{mn}\left(\underline{Y}\right) T_n - \sum_{n=N_1+1}^{N} B_{mn}\left(\underline{Y}\right) \Phi_n \\ &= \sum_{n=1}^{N_1} B_{mn}\left(\underline{Y}\right) \widetilde{\Phi}_n - \sum_{n=N_1+1}^{N} A_{mn}\left(\underline{Y}\right) \widetilde{T}_n, \quad m = 1, \ldots, N, \end{aligned} \tag{18}$$

then the calculated temperatures T_n, $n = 1, \ldots, N_1$, on the known boundary Γ_1 and fluxes Φ_n, $n = (N_1 + 1), \cdots, N$, on the unknown boundary Γ_2 are functions of the unknown parameters given by the vector $\underline{Y}$, i.e.,

$$\begin{aligned} T_n &= T_n\left(\underline{Y}\right), \quad n = 1, \ldots, N_1, \\ \Phi_n &= \Phi_n\left(\underline{Y}\right), \quad n = (N_1 + 1), \ldots, N. \end{aligned} \tag{19}$$

The numerical scheme proposed in this study is based on the minimisation of the Tikhonov functional

$$\mathcal{F}_\lambda(\cdot) : \mathbb{R}^{2(N_2-1)} \longrightarrow [0,\infty)$$
$$\mathcal{F}_\lambda\left(\underline{Y}\right) = \frac{1}{2}\|T^{(\text{num})}\left(\underline{Y}\right)|_{\Gamma_1} - \widetilde{T}^{\varepsilon}|_{\Gamma_1}\|_2^2 + \lambda \sum_{n=N_1+1}^{N} \|\underline{y}^{(n)} - \underline{y}^{(n-1)}\|_2^2 \tag{20}$$

with respect to the vector $\underline{Y} = \left(\underline{y}^{(N_1+1)}, \ldots, \underline{y}^{(N-1)}\right)^{\text{T}} \in \mathbb{R}^{2(N_2-1)}$, provided that an initial guess $\underline{Y}^{(0)} \in \mathbb{R}^{2(N_2-1)}$ is given, where $\lambda > 0$ is a regularization parameter to be prescribed, $T^{(\text{num})}\left(\underline{Y}\right)|_{\Gamma_1} = \left(T_1\left(\underline{Y}\right), \ldots, T_{N_1}\left(\underline{Y}\right)\right)^{\text{T}}$ is the vector containing the calculated values of the temperature on Γ_1 and $\widetilde{T}^{\varepsilon}|_{\Gamma_1}$ represents a noisy measurement data for the exact data $\widetilde{T}|_{\Gamma_1}$.

In the case of the problem given by Eqs. (1), (9) and (10_2), it should be noted that the discretised BEM system of Eqs. (16) is regarded as the solution of a direct problem with the boundary conditions $T(\underline{x}) = \widetilde{T}(\underline{x})$, $\underline{x} \in \Gamma_1$ and $\Phi(\underline{x}) = \widetilde{\Phi}(\underline{x})$, $\underline{x} \in \Gamma_2$, whilst the objective function $\mathcal{F}$ minimises the difference between the calculated $\Phi^{(\text{num})}\left(\underline{Y}\right)|_{\Gamma_1} = \left(\Phi_1\left(\underline{Y}\right), \ldots, \Phi_{N_1}\left(\underline{Y}\right)\right)^{\text{T}}$ and the measured noisy fluxes $\widetilde{\Phi}^{\varepsilon}|_{\Gamma_1}$ on the known boundary Γ_1, namely

$$\mathcal{F}_\lambda(\cdot) : \mathbb{R}^{2(N_2-1)} \longrightarrow [0,\infty)$$
$$\mathcal{F}_\lambda\left(\underline{Y}\right) = \frac{1}{2}\|\Phi^{(\text{num})}\left(\underline{Y}\right)|_{\Gamma_1} - \widetilde{\Phi}^{\varepsilon}|_{\Gamma_1}\|_2^2 + \lambda \sum_{n=N_1+1}^{N} \|\underline{y}^{(n)} - \underline{y}^{(n-1)}\|_2^2. \tag{21}$$

Numerically, the objective functional (20) or (21) is minimised using the NAG subroutine E04UPF, which is designed to minimise an arbitrary smooth sum of squares subject to constraints. This may include simple bounds on the variables, linear constraints and smooth nonlinear constraints. Each iteration of the subroutine includes the following: (a) the solution of a quadratic programming subproblem; (b) a line search with an augmented Lagrangian function; and (c) a quasi-Newton update of the approximate Hessian of the Lagrangian function, for more details see Gill et al. [37]. The gradient of the objective functional (20) or (21) has been calculated using forward finite differences with a step of 10^{-3} which was found to be sufficiently small that a further decrease in this value does not affect significantly the accuracy of the numerical results.

5 Numerical results and discussion

In this section, we consider the case when the unknown boundary Γ_2 is the graph of an unknown function $f : [-R, R] \longrightarrow \mathbb{R}$, $R > 0$, taking the x_1-axis to pass through the endpoints $f(-R) = f(R) = 0$ and fixing the origin at $x_1 = 0$. Therefore, the endpoints of the boundary elements Γ_n on Γ_2 will have the known equally-spaced x_1-coordinates $y_1^{(n)} = R(2n-N-N_1)/(N-N_1)$ for $n = N_1, \ldots, N$. Furthermore, since $f(-R) = f(R) = 0$, the functional (20) will depend on only $(N_2 - 1)$ unknowns, namely $y_2^{(N_1+1)}, \ldots, y_2^{(N-1)}$, where $y_2^{(n)} = f(y_1^{(n)})$ for $n = (N_1 + 1), \ldots, (N - 1)$. Consequently, the functional (20) has the following form:

$$\mathcal{F}_\lambda(\cdot) : \mathbb{R}^{N_2-1} \longrightarrow [0,\infty)$$
$$\mathcal{F}_\lambda\left(\underline{Y}\right) = \frac{1}{2}\|T^{(\text{num})}\left(\underline{Y}\right)|_{\Gamma_1} - \widetilde{T}^{\varepsilon}|_{\Gamma_1}\|_2^2 + \lambda\|\underline{Y}'\|_2^2$$
$$= \frac{1}{2}\sum_{n=1}^{N_1}\left(T_n\left(\underline{Y}\right) - \widetilde{T}_n^{\varepsilon}\right)^2 + \lambda\Big\{\left(y_2^{(N_1+1)}\right)^2 + \sum_{n=N_1+2}^{N-1}\left(y_2^{(n)} - y_2^{(n-1)}\right)^2 + \left(y_2^{(N-1)}\right)^2\Big\}, \tag{22}$$

where we have stopped penalising the x_1-coordinates in the norms $\|\underline{y}^{(n)} - \underline{y}^{(n-1)}\|_2^2$ since they are known. On assuming that the unknown boundary Γ_2 is located below the x_1-axis and an a priori estimate $l_{\max} > 0$ for the size of the solution domain Ω is available, the following simple bounds are imposed for the components of the unknown vector $\underline{Y} = \left(\underline{y}^{(N_1+1)}, \ldots, \underline{y}^{(N-1)}\right)^{\text{T}} \in \mathbb{R}^{2(N_2-1)}$

$$-l_{\max} \le \underline{y}^{(n)} \le 0, \quad n = (N_1 + 1), \ldots, (N - 1), \tag{23}$$

where the values for the estimate $l_{\max} > 0$ will be mentioned later. It should be noted that the zeroth-order regularization procedure based on penalising the norm of the solution $\underline{Y}$, rather than its derivative $\underline{Y}'$, did not produce sufficiently accurate and stable numerical results and this conclusion is in accordance with the results obtained by Peneau et al. [38], Lesnic et al. [23] and Marin and Lesnic [24] who have solved a similar problem for the Laplace equation and the Lamé system, respectively. Therefore, the assumption of smoothness of the numerical solution for Γ_2, as given by the first-order Tikhonov functional (22), is essential in order to obtain an accurate and stable numerical solution. Alternatively, instead of employing the functional (22), one may parameterise the unknown boundary Γ_2 with various approximating functions and the problem reduces to determining the coefficients of the approximation, see Birginie et al. [39].

In order to present the performance of the numerical method proposed, we solve the inverse geometric problem (1), (9) and (10_1) for the modified Helmholtz equation, i.e. $\mathcal{L} = \Delta - k^2$, $k > 0$, in the following two-dimensional geometries which are schematically presented in Figures 1a–d:

Example 1 We consider the unit disk $\Omega = \left\{\underline{x} = (x_1, x_2) \;\middle|\; x_1^2 + x_2^2 < R^2\right\}$, $R = 1.0$, whose boundary Γ consists of two parts, namely

$$\Gamma_1 = \left\{\underline{x} = (x_1, x_2) \;\middle|\; x_2 = \sqrt{R^2 - x_1^2},\ -R \le x_1 \le R\right\}, \tag{24}$$

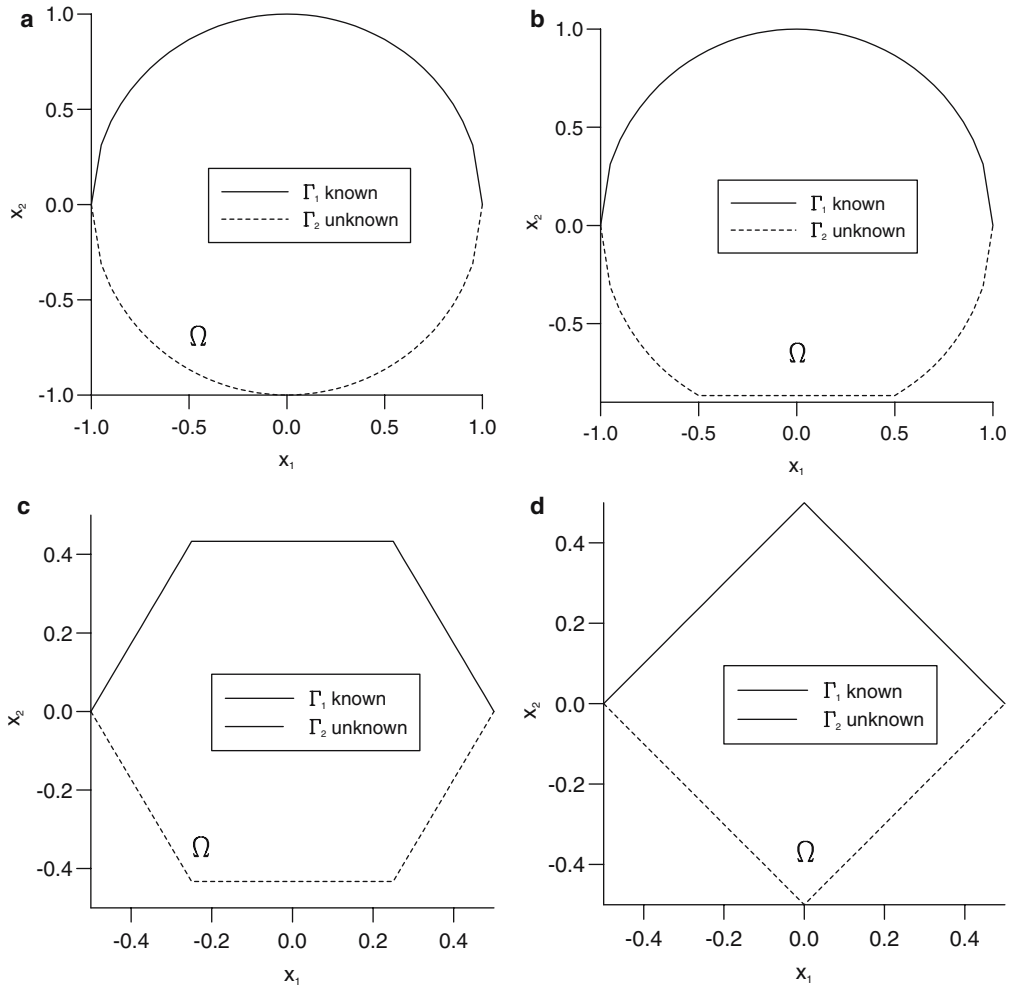

Fig. 1 A schematic diagram of the domain Ω, the known and the unknown boundaries Γ_1 and Γ_2, respectively, for the inverse geometric problem corresponding to examples (a) 1, (b) 2, (c) 3, and (d) 4

$$\Gamma_2 = \Gamma \setminus \Gamma_1 = \left\{ \underline{x} = (x_1, x_2) \,\middle|\, x_2 = -\sqrt{R^2 - x_1^2},\ -R < x_1 < R \right\}. \tag{25}$$

Example 2 We consider the domain Ω which is bounded by the following curves

$$\Gamma_1 = \left\{ \underline{x} = (x_1, x_2) \,\middle|\, x_2 = \sqrt{R^2 - x_1^2},\ -R \le x_1 \le R \right\}, \quad R = 1.0, \tag{26}$$

$$\begin{aligned}\Gamma_2 = \Gamma \setminus \Gamma_1 &= \left\{ \underline{x} = (x_1, x_2) \,\middle|\, x_2 = -\sqrt{R^2 - x_1^2}, -R < x_1 < -R/2 \right\} \\ &\cup \left\{ \underline{x} = (x_1, x_2) \,\middle|\, x_2 = -R\sqrt{3}/2, -R/2 \le x_1 \le R/2 \right\} \\ &\cup \left\{ \underline{x} = (x_1, x_2) \,\middle|\, x_2 = -\sqrt{R^2 - x_1^2},\ R/2 < x_1 < R \right\}.\end{aligned} \tag{27}$$

Example 3 We consider the hexagon Ω which is enclosed in the circle $B(0, R)$ and is bounded by the following curves

$$\begin{aligned}\Gamma_1 &= \left\{ \underline{x} = (x_1, x_2) \,\middle|\, x_2 = (R - x_1)\sqrt{3},\ R/2 < x_1 < R \right\} \\ &\cup \left\{ \underline{x} = (x_1, x_2) \,\middle|\, x_2 = R\sqrt{3}/2,\ -R/2 \le x_1 \le R/2 \right\} \\ &\cup \left\{ \underline{x} = (x_1, x_2) \,\middle|\, x_2 = (R + x_1)\sqrt{3}, -R < x_1 < -R/2 \right\}, \quad R = 0.5,\end{aligned} \tag{28}$$

$$\begin{aligned}\Gamma_2 = \Gamma \setminus \Gamma_1 &= \left\{ \underline{x} = (x_1, x_2) \,\middle|\, x_2 = -(R + x_1)\sqrt{3}, -R < x_1 < -R/2 \right\} \\ &\cup \left\{ \underline{x} = (x_1, x_2) \,\middle|\, x_2 = -R\sqrt{3}/2, -R/2 \le x_1 \le R/2 \right\} \\ &\cup \left\{ \underline{x} = (x_1, x_2) \,\middle|\, x_2 = -(R - x_1)\sqrt{3}, R/2 < x_1 < R \right\}.\end{aligned} \tag{29}$$

Example 4 We consider the domain Ω as the square $\left(-R/\sqrt{2},\ R/\sqrt{2}\right)^2$ rotated by an angle $\theta = \pi/4$ about the origin O which is bounded by the following curves

$$\Gamma_1 = \left\{\underline{x} = (x_1, x_2) \mid x_2 = R - x_1,\ 0 \le x_1 \le R\right\} \cup \left\{\underline{x} = (x_1, x_2) \mid x_2 = R + x_1,\ -R \le x_1 \le 0\right\}, \quad R = 0.5, \tag{30}$$

$$\Gamma_2 = \Gamma \setminus \Gamma_1 = \left\{\underline{x} = (x_1, x_2) \mid x_2 = -(R + x_1),\ -R < x_1 \le 0\right\} \cup \left\{\underline{x} = (x_1, x_2) \mid x_2 = -(R - x_1),\ 0 \le x_1 < R\right\}. \tag{31}$$

For the examples investigated herein, we consider the following analytical solution for the temperature

$$T^{(\mathrm{an})}(\underline{x}) = \exp\left(a_1 x_1 + a_2 x_2\right), \quad \underline{x} = (x_1, x_2) \in \Omega, \tag{32}$$

where $a_1 = 0.5$, $a_2 = \sqrt{k^2 - a_1^2}$ and $k = 2.0$, whilst the analytical flux on the boundary Γ is given by

$$\Phi^{(\mathrm{an})}(\underline{x}) = \exp\left(a_1 x_1 + a_2 x_2\right)\left[a_1 \nu_1(\underline{x}) + a_2 \nu_2(\underline{x})\right], \quad \underline{x} = (x_1, x_2) \in \Gamma, \tag{33}$$

whilst the a priori estimate $l_{\max} > 0$ for the size of the solution domain Ω was taken to be $l_{\max} = 2R$.

It should be noted that we may create boundary data which are exempt from any numerical noise even when analytical expressions for the temperature and the flux are available and, in what follows, they will be referred to as "exact data". For example, exact data can be obtained by solving the following mixed boundary value problem

$$\begin{cases} \mathcal{L}T(\underline{x}) \equiv \left(\Delta - k^2\right) T(\underline{x}) = 0, & \underline{x} \in \Omega \\ \Phi(\underline{x}) = \Phi^{(\mathrm{an})}(\underline{x}), & \underline{x} \in \Gamma_1 \\ T(\underline{x}) = T^{(\mathrm{an})}(\underline{x}), & \underline{x} \in \Gamma_2. \end{cases} \tag{34}$$

Hence the inverse geometric problem under investigation is given by Eqs. (1), (9) and (10_1) in which the input temperature $\widetilde{T}|_{\Gamma_2} = T^{(\mathrm{an})}|_{\Gamma_2}$ and flux $\widetilde{\Phi}|_{\Gamma_1} = \Phi^{(\mathrm{an})}|_{\Gamma_1}$ data are given by relations (32) and (33), respectively, and the input temperature datum $\widetilde{T}|_{\Gamma_1}$ is given by solving numerically the mixed boundary value problem (34).

The examples described above have been chosen in order to test the performance of the numerical method proposed for both a smooth curve, e.g., example 1, and a piecewise smooth curve with corner(s), e.g., examples 2–4, see also Fig. 1. The numerical results presented in this section have been obtained using a discretisation of the boundaries Γ, Γ_1 and Γ_2 with $N_1 = N_2 = 20$ boundary elements for examples 1, 2 and 4, and $N_1 = N_2 = 30$ boundary elements for example 3, such that $N = N_1 + N_2$. These values were found to be sufficiently large such that any further refinement of the mesh size did not significantly improve the accuracy of the numerical results.

Exact data are seldom available in practice since measurement errors always include noise in the prescribed boundary conditions. In order to investigate the stability of the numerical method proposed, the Cauchy boundary data $\widetilde{T}|_{\Gamma_1}$ and/or $\widetilde{\Phi}|_{\Gamma_1}$ have been perturbed as

$$\widetilde{T}^{\varepsilon}|_{\Gamma_1} = \widetilde{T}|_{\Gamma_1} + \delta\widetilde{T}, \quad \delta\widetilde{T} = \mathrm{G05DDF}(0, \sigma_T), \quad \sigma_T = \max_{\Gamma_1}|\widetilde{T}| \times \frac{p}{100},$$
$$\widetilde{\Phi}^{\varepsilon}|_{\Gamma_1} = \widetilde{\Phi}|_{\Gamma_1} + \delta\widetilde{\Phi}, \quad \delta\widetilde{\Phi} = \mathrm{G05DDF}(0, \sigma_\Phi), \quad \sigma_\Phi = \max_{\Gamma_1}|\widetilde{\Phi}| \times \frac{p}{100}, \tag{35}$$

where $\delta\widetilde{T}$ and $\delta\widetilde{\Phi}$ are Gaussian random variables with mean zero and standard deviations σ_T and σ_Φ, respectively, generated by the NAG subroutine G05DDF, and $p \in \{1, 2, 3\}$ is the percentage of additive noise included into the input data $\widetilde{T}|_{\Gamma_1}$ and/or $\widetilde{\Phi}|_{\Gamma_1}$ in order to simulate the inherent measurement errors.

In the inverse analysis of retrieving the unknown boundary Γ_2, the initial guess $\underline{Y}^{(0)} \in \mathbb{R}^{2(N_2-1)}$ for the minimisation of the objective functional (22) has been taken, for simplicity, to be zero. Although not presented in this paper, it should be noted that the numerical algorithm described in Sect. 4 has been found to be robust by producing the same numerical convergent results for other initial guesses. In order to study the convergence of the numerical method employed, we consider the accuracy error defined by

$$E_Y = ||\underline{Y}_\lambda - \underline{Y}^{(\mathrm{ex})}||_2, \tag{36}$$

where $\underline{Y}^{(\mathrm{ex})}$ and $\underline{Y}_\lambda$ are vectors containing the exact and the numerical values corresponding to a specified value of the regularization parameter λ for the coordinates of the unknown boundary Γ_2, respectively. Figs. 2(a) and (b) present the accuracy error E_Y defined by relation (36), as a function of the regularization parameter λ obtained for the inverse problem given by examples 1 and 2, respectively, for various levels of noise added into the input temperature data $\widetilde{T}|_{\Gamma_1}$. From these figures it can be seen that for the error E_Y to attain its minimum requires the optimal value λ_{opt} of the regularization parameter λ to be chosen when using the Tikhonov regularization method and this will be discussed later. Moreover, the minimum value of E_Y decreases as the noise added into the input data decreases.

In the functional (22), the choice of the optimal regularization parameter $\lambda = \lambda_{\mathrm{opt}}$ is essential in order to achieve the stability on the numerical solution. In this study, we have used an L-curve type criterion, see Hansen [30], which plots on a log-log scale the least-squares gap, i.e., the error $E_T = ||T^{(\mathrm{num})}(\underline{Y})|_{\Gamma_1} - T^{(\mathrm{an})}|_{\Gamma_1}||_2$, versus the norm of the derivative of the solution, $||\underline{Y}'||_2$, for various values of the regularization parameter λ. As with every practical method, the L-curve method has its advantages and disadvantages. It should be noted that there are two main disadvantages/limitations of the L-curve criterion and understanding these is the key to the proper use of the L-curve criterion. The first disadvantage is related to the reconstruction of very smooth exact solutions, see Tikhonov et al. [40] and Hansen [41]. Hanke [42] has shown that the L-curve criterion fails for such solutions and the smoother the solution the worse the regularization parameter computed using the L-curve criterion. In fact, for exact input displacement data, i.e., $p = 0$, we have not obtained any L-curve. However, it is not clear

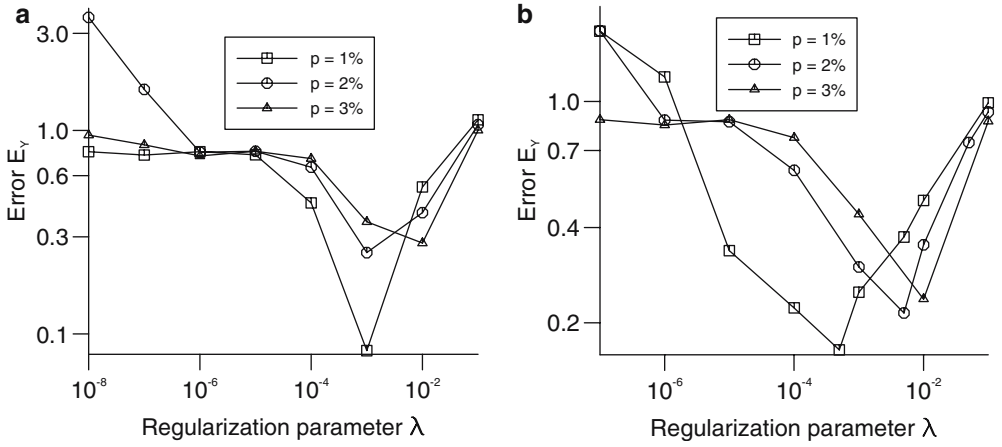

Fig. 2 The error $E_Y = ||\underline{Y}_\lambda - \underline{Y}^{(\mathrm{ex})}||_2$, as a function of the regularization parameter λ, obtained for the examples (a) 1, and (b) 2

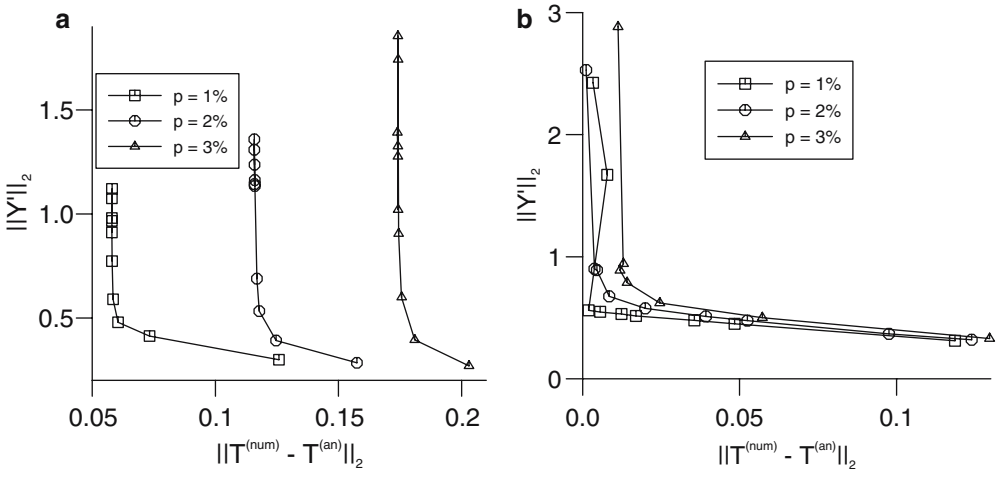

Fig. 3 The L-curves obtained with various levels of noise added into the temperature data $T^{(\mathrm{an})}|_{\Gamma_1}$, for the examples (a) 1, and (b) 2

how often very smooth solutions arise in practical problems and therefore the input data used is considered to be noisy, i.e., $p > 0$. The second limitation of the L-curve criterion is concerned with its asymptotic behaviour as the problem size, N, increases. Vogel [43] has shown that the regularization parameter, λ, computed using the L-curve criterion may not behave consistently with the optimal regularization parameter, λ_{opt}, as the problem size increases. However, the situation in which the same problem is discretised for increasing N, may not occur so often in practice. In practical applications the problem size, N, is fixed by a particular measurement setup and if a larger N is required then a new experiment has to be performed. The main advantages of the L-curve criterion are its robustness and its ability to treat perturbations consisting of correlated noise, see Hansen [41].

In Figs. 3(a) and (b) we present the L-curve plots for the examples 1 and 2, respectively, obtained for various levels of noise added into the input temperature data $\widetilde{T}|_{\Gamma_1}$, namely $p \in \{1, 2, 3\}$. The optimal values, λ_{opt}, of the regularization parameter, λ, are chosen at the corners of these curves in order to balance the under-smooth regions, i.e., λ too small, and the over-smooth regions, i.e., λ too large. A more systematic way to find this corner is to determine the maximum point of the curvature of the L-curve with respect to the regularization parameter, $\lambda > 0$, for more details on this method we refer the reader to Hansen [30,41] and Hansen and O'Leary [44]. Alternatively to this heuristical method, one may use other more rigorous criteria, such as the discrepancy principle, see Morozov [31], or the generalised cross-validation principle, see Wahba [32]. However, Figures 3(a) and (b) illustrate clearly the L-shaped curves and therefore the L-curve criterion is applicable.

The optimal values, λ_{opt}, of the regularization parameter, λ, obtained for the examples considered in this study with various levels of noise added into the input temperature data $\widetilde{T}|_{\Gamma_1}$ are showed in Table 1 which also presents the corresponding values of the accuracy error, E_Y, and the objective functional, $\mathcal{F}_\lambda$, and the number of iterations, n, performed. From Table 1 it can be seen that the values of the error E_Y defined by relation (36) and the objective functional $\mathcal{F}_\lambda$ given by equation (22), decrease as the level of noise added into the input temperature data decreases. Moreover, the number

Table 1 The values of the error E_Y, the objective functional $\mathcal{F}_\lambda$ and the number of iterations performed n, obtained for the optimal regularization parameter λ_{opt} and various levels of noise p added into the input temperature data $T^{(\text{an})}|_{\Gamma_1}$

	p (%)	λ_{opt}	$E_Y(\lambda_{\text{opt}})$	$\mathcal{F}_{\lambda_{\text{opt}}}$	n_{opt}
Example 1	1	1.0×10^{-3}	0.8294×10^{-1}	0.1909×10^{-3}	20
	2	1.0×10^{-3}	0.2511×10^{0}	0.2847×10^{-3}	21
	3	1.0×10^{-2}	0.2796×10^{0}	0.1944×10^{-2}	22
Example 2	1	5.0×10^{-4}	0.1643×10^{0}	0.7641×10^{-4}	15
	2	5.0×10^{-3}	0.2148×10^{0}	0.7697×10^{-3}	18
	3	1.0×10^{-2}	0.2376×10^{0}	0.1635×10^{-2}	18
Example 3	1	1.0×10^{-3}	0.1219×10^{0}	0.1299×10^{-3}	95
	2	7.5×10^{-3}	0.1321×10^{0}	0.1383×10^{-3}	111
	3	1.0×10^{-2}	0.1556×10^{0}	0.1972×10^{-3}	113
Example 4	1	1.0×10^{-3}	0.1268×10^{0}	0.2412×10^{-4}	65
	2	5.0×10^{-3}	0.1401×10^{0}	0.1283×10^{-3}	79
	3	5.0×10^{-3}	0.1445×10^{0}	0.1197×10^{-3}	92

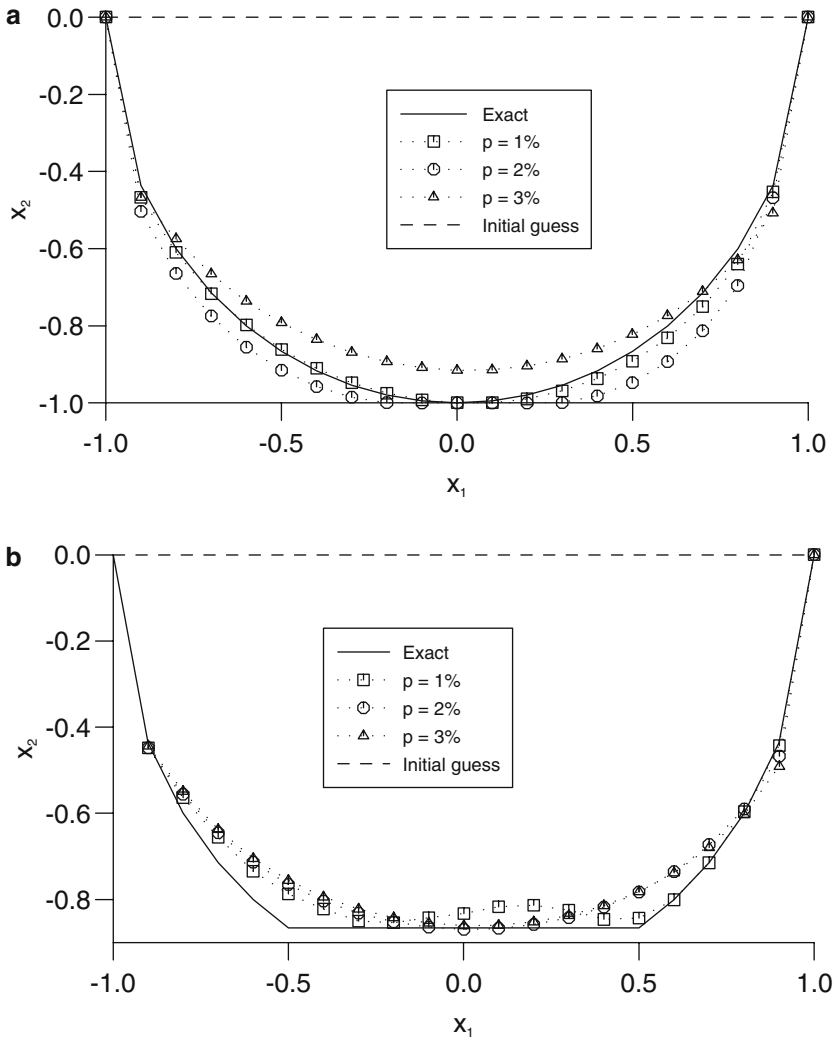

Fig. 4 The exact (—), the initial guess (− −) and the numerical solution for the unknown boundary Γ_2, obtained with various levels of noise added into the temperature data $T^{(\text{an})}|_{\Gamma_1}$, for the examples (a) 1, and (b) 2

of iterations n performed in order to minimise the objective functional (22) increases as the level of noise added into the input temperature data increases.

Figures 4(a) and (b) illustrate the initial guess, the exact and the numerical values for the unknown boundary Γ_2 obtained using the optimal regularization parameter $\lambda = \lambda_{\text{opt}}$

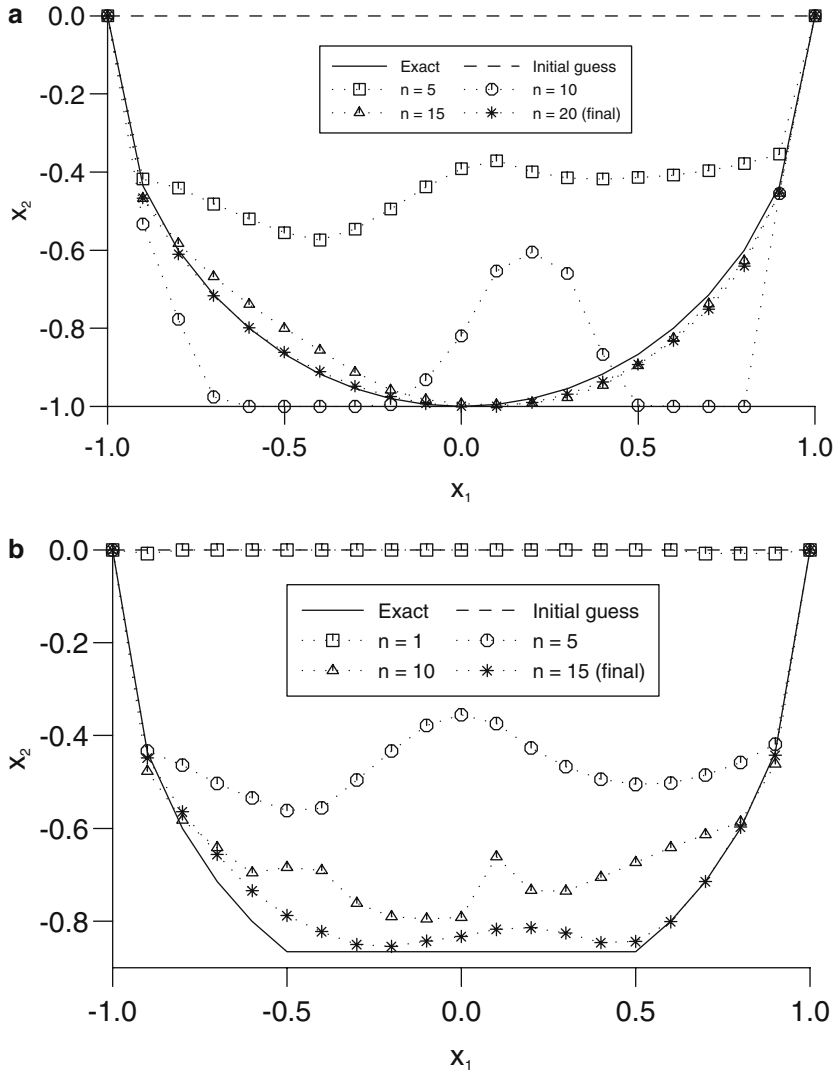

Fig. 5 The iterative convergence process for the unknown boundary Γ_2 as the initial guess $(- -)$ moves towards the target $(—)$, obtained with $p = 1\%$ noise added into the temperature data $T^{(\mathrm{an})}|_{\Gamma_1}$ and various numbers of iterations performed, for the examples (a) 1, and (b) 2

chosen according to the L-curve criterion and various levels of noise added into the input temperature data $\widetilde{T}|_{\Gamma_1}$, namely $p \in \{1, 2, 3\}$, for the problems given by examples 1 and 2, respectively. From Figs. 4(a) and (b) and Table 1 it can be seen that for both examples the numerical solutions are stable and consistent with the amount of noise p added into the input data $\widetilde{T}|_{\Gamma_1}$. Moreover, they converge to their corresponding exact targets Γ_2, given by equations (25) and (27), as the amount of noise p decreases, i.e. as the data errors tend to zero. Thus, the numerical solution is convergent to the exact solution.

Figures 5(a) and (b) show the iterative convergence process for the unknown boundary Γ_2 as the initial guess moves towards the target when obtained for $p = 1\%$ noise added into the temperature data $\widetilde{T}|_{\Gamma_1}$, $\lambda = \lambda_{\mathrm{opt}}$ according to the L-curve criterion and various numbers of iterations performed for the examples 1 and 2, respectively. It can be seen from these figures that the numerical results for the unknown boundaries given by equations (25) and (27) are reasonable approximations of their exact values after a small number of iterations, e.g., $n = 15$ iterations in the case of example 1 and $n = 10$ iterations in the case of example 2. It should be noted that the final numerical results for the unknown boundaries (25) and (27) are obtained after $n_{\mathrm{opt}} = 20$ and $n_{\mathrm{opt}} = 15$ iterations for examples 1 and 2, respectively, see Table 1.

The importance of the choice of the optimal regularization parameter λ_{opt} is illustrated in Figs. 6(a) and (b) which present the exact values in comparison with the numerical solutions corresponding to different values of the regularization parameter, namely $\lambda < \lambda_{\mathrm{opt}}$, $\lambda = \lambda_{\mathrm{opt}}$ and $\lambda > \lambda_{\mathrm{opt}}$, for the unknown boundaries given by relations (25) and (27), respectively. From Figs. 6(a) and (b), it can be seen that if the regularization parameter λ is taken to be too small then it produces oscillatory numerical solutions which are dominated by the contributions from the data errors, whilst if the regularization parameter λ is taken to be too large then it produces

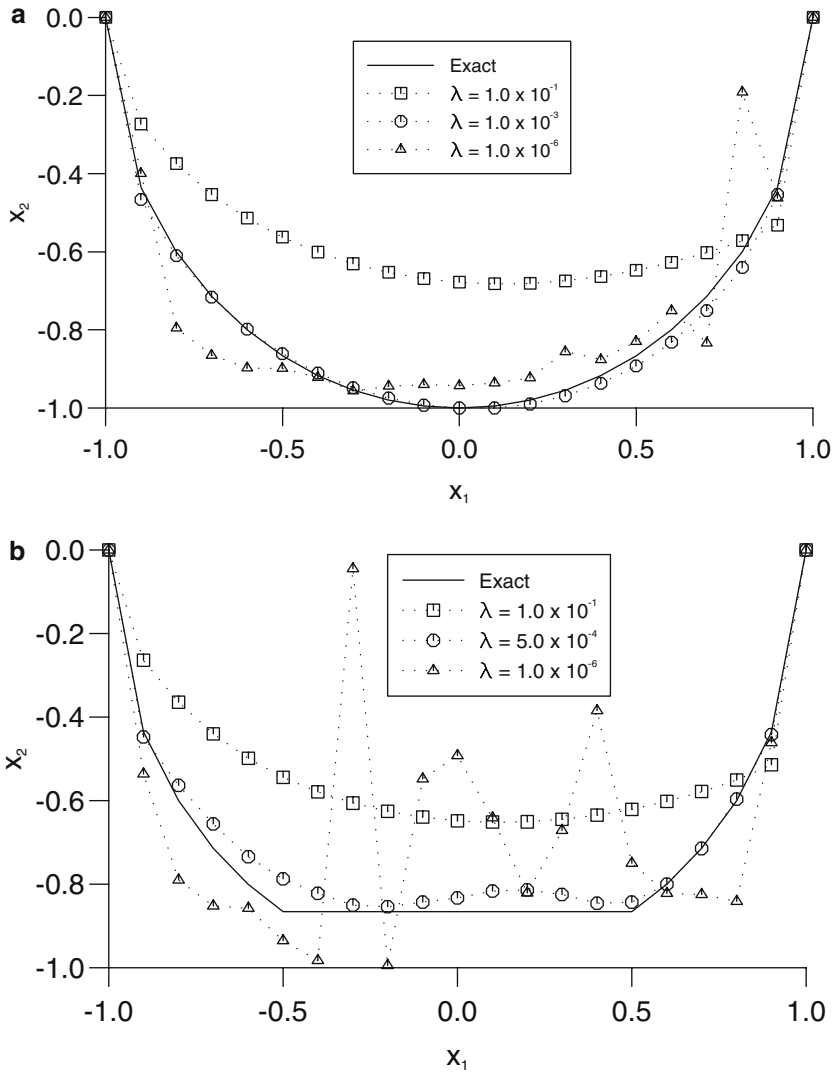

Fig. 6 The exact (—) and the numerical solution for the unknown boundary Γ_2, obtained with $p = 1\%$ noise added into the temperature data $T^{(\mathrm{an})}|_{\Gamma_1}$ and various values of the regularization parameter λ, namely $\lambda < \lambda_{rmopt}$, $\lambda = \lambda_{\mathrm{opt}}$ and $\lambda > \lambda_{\mathrm{opt}}$, for the examples (a) 1, and (b) 2

over-smooth numerical solutions which do not fit the given data, as discussed before.

The numerical algorithm described in Sect. 4 produces stable and consistent numerical solutions with respect to the amount of noise added into the input temperature data $\widetilde{T}|_{\Gamma_1}$ also in the case of piecewise smooth geometries with corners. Figs. 7(a) and (b) illustrate the initial guess, the exact and the numerical values for the unknown boundary Γ_2 obtained using the optimal regularization parameter $\lambda = \lambda_{\mathrm{opt}}$ chosen according to the L-curve criterion and various levels of noise added into the input data $\widetilde{T}|_{\Gamma_1}$, namely $p \in \{1, 2, 3\}$, for the problems given by examples 3 and 4, respectively. It can be seen from these figures and Table 1 that the numerical solutions retrieved for the two piecewise smooth geometries investigated converge to their corresponding exact targets Γ_2, given by Eqs. (29) and (31), as the amount of noise p decreases, i.e., as the data errors tend to zero and hence the numerical solution is convergent to the exact solution. However, it can be noted from Fig. 7 that for both examples 3 and 4 the corner points are, as expected, rounded-off since the minimisation of the first-order regularization Tikhonov functional (22) subject to the simple bounds (23) imposes the numerical solution to be smooth.

The sensitivity of the numerical results obtained using the proposed method with respect to the type of perturbed boundary condition on Γ_1 is analysed next. To do so, we consider the inverse geometric problem (1), (9) and (10_1) for the modified Helmholtz equation corresponding to examples 1 and 4 for a fixed level of noise ($p = 1\%$) added into either the temperature or the flux data on the known boundary Γ_1. Figures 8(a) and (b) show the initial guess, the exact and the numerical values for the unknown boundary Γ_2 obtained using the optimal regularization parameter $\lambda = \lambda_{\mathrm{opt}}$ as given by the L-curve criterion, and noisy input temperature $\widetilde{T}^{\varepsilon}|_{\Gamma_1}$ and flux data $\widetilde{\Phi}^{\varepsilon}|_{\Gamma_1}$ data, according to equation (35), for the

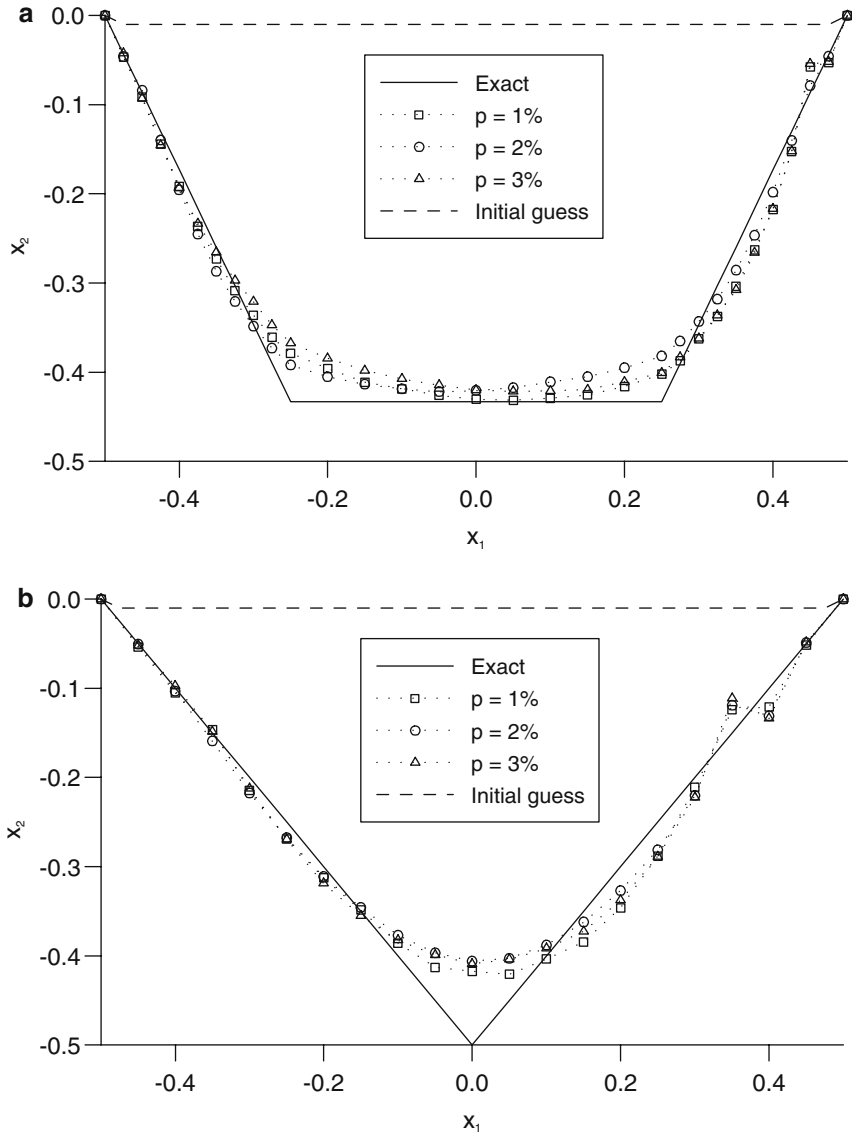

Fig. 7 The exact (—), the initial guess (– –) and the numerical solution for the unknown boundary Γ_2, obtained with various levels of noise added into the temperature data $T^{(an)}|_{\Gamma_1}$, for the examples (a) 3, and (b) 4

problems given by examples 1 and 4, respectively. As expected, the numerical solution retrieved when using $p = 1\%$ noise added into the input temperature data $\widetilde{T}|_{\Gamma_1}$ is a better approximate for the unknown boundary Γ_2 than the numerical solution obtained for the same amount of noise added into the input flux data $\widetilde{\Phi}|_{\Gamma_1}$ since the expression for the flux contains higher-order derivatives of the temperature. Although not presented herein, it is reported that similar results have been obtained for the other examples analysed in this paper, as well as the Helmholtz equation.

6 Conclusions

In this paper, we have investigated the identification of an unknown part of the boundary of a two-dimensional domain in which Helmholtz-type equations are satisfied from additional Cauchy data on the remaining known portion of the boundary of the solution domain. This inverse problem has been approached using the Tikhonov first-order regularization procedure combined with the boundary element method, whilst the regularization parameter has been chosen according to the L-curve criterion, although one may use the Morozov discrepancy principle or the generalised cross-validation principle. From the numerical results obtained for various levels of noise added into the input data, it can be concluded that the numerical method proposed produces very accurate and stable numerical solutions for the unknown part of the boundary, as the amount of noise added into the input data decreases. Moreover, the regularization method proposed in this study can be extended to three-dimensional Helmholtz-type equations, as well as two- and three-dimensional Helmholtz-type equations with

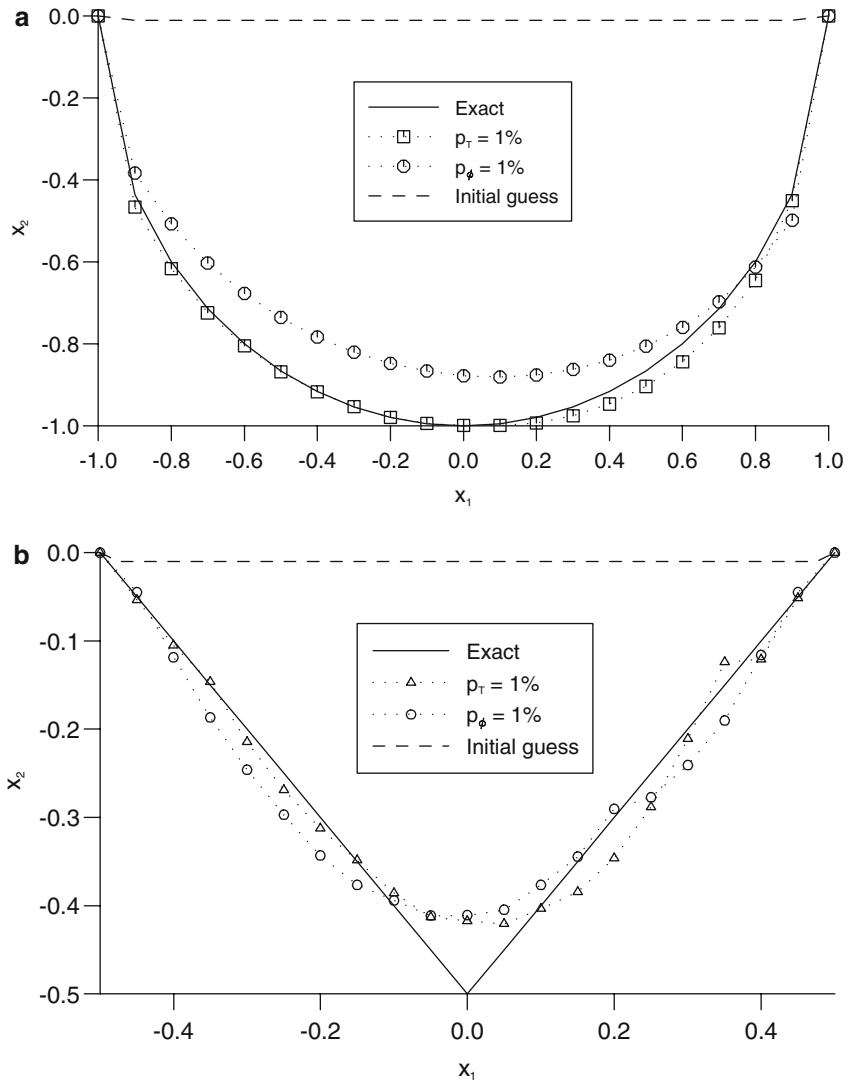

Fig. 8 The exact (—), the initial guess (– –) and the numerical solution for the unknown boundary Γ_2, obtained with $p = 1\%$ noise added into the temperature $T^{(\mathrm{an})}|_{\Gamma_1}$ and the flux data $\Phi^{(\mathrm{an})}|_{\Gamma_1}$, for the examples (a) 1, and (b) 4

space-dependent coefficients, but these are deferred as future work.

A Integration constants for Helmholtz-type equations: Constant boundary elements

Here we describe the type boundary elements employed, as well as the NAG subroutines used for the computation of the BEM matrices A and B given by Eq. (15), in the case of two-dimensional Helmholtz-type equations.

A.1 Geometry of the boundary elements

The boundary elements $\Gamma^{(n)}$, $n = 1, \ldots, N$, are straight line segments, see Fig. 9, parametrised as

$$\underline{y}(\cdot) : [0, 1] \longrightarrow \Gamma^{(n)} = \left[\underline{y}^{(n-1)}, \underline{y}^{(n)}\right],$$
$$\underline{y}(t) = \left(\underline{y}^{(n)} - \underline{y}^{(n-1)}\right) t + \underline{y}^{(n-1)}. \qquad \text{(A1)}$$

Consequently, the vector $\underline{r}\left(\underline{x}, \underline{y}\right)$ determined by the positions of the collocation point $\underline{x} \in \overline{\Omega}$ and any point $\underline{y}$ located on the boundary element $\Gamma^{(n)}$ can be expressed as

$$\underline{r}\left(\underline{x}, \underline{y}(t)\right) = \underline{y}(t) - \underline{x} = \underline{a}^n\, t - \underline{c}^n(\underline{x}),$$
$$\underline{a}^n = \underline{y}^{(n)} - \underline{y}^{(n-1)}, \quad \underline{c}^n(\underline{x}) = \underline{x} - \underline{y}^{(n-1)}, \qquad \text{(A2)}$$

or by components

$$r_j\left(\underline{x}, \underline{y}(t)\right) = y_j(t) - x_j = a_j^n\, t - c_j^n(\underline{x}),$$
$$a_j^n = y_j^{(n)} - y_j^{(n-1)}, \quad c_j^n(\underline{x}) = x_j - y_j^{(n-1)}, \quad j = 1, 2. \qquad \text{(A3)}$$

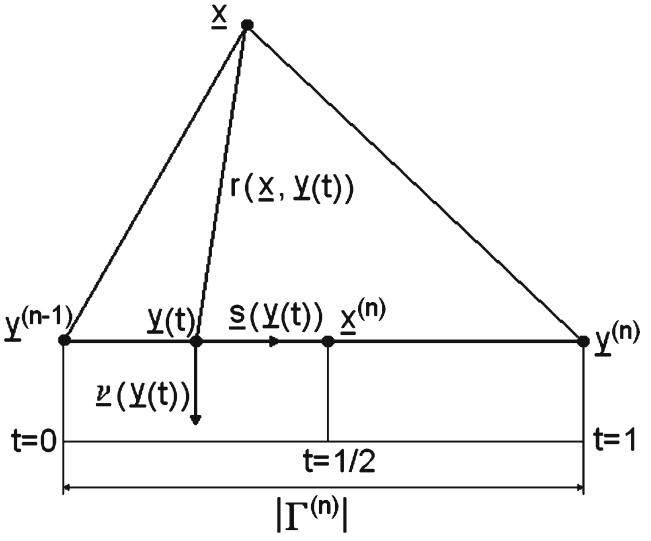

Fig. 9 General geometry at the collocation point $\underline{x}$ when the integration is performed over the boundary element $\Gamma^{(n)} = \left[\underline{y}^{(n-1)}, \underline{y}^{(n)}\right]$

On using the formulae$(A1)$–$(A3)$, the following expressions are obtained for the Euclidean norm $r\left(\underline{x}, \underline{y}\right)$ of the vector $\underline{r}\left(\underline{x}, \underline{y}\right)$

$$r\left(\underline{x}, \underline{y}(t)\right) = \left\|\underline{r}\left(\underline{x}, \underline{y}(t)\right)\right\|_2 = \sqrt{a^n\, t^2 + b^n(\underline{x})\, t + c^n(\underline{x})}, \tag{A4}$$

and the differential $\mathrm{d}\Gamma(\underline{y})$

$$\mathrm{d}\Gamma(\underline{y}(t)) = \sqrt{\left(\frac{\mathrm{d}y_1(t)}{\mathrm{d}t}\right)^2 + \left(\frac{\mathrm{d}y_2(t)}{\mathrm{d}t}\right)^2}\,\mathrm{d}t = \sqrt{a^n}\,\mathrm{d}t, \tag{A5}$$

respectively, where

$$\begin{aligned} a^n &= \underline{a}^n \cdot \underline{a}^n = \left(a_1^n\right)^2 + \left(a_2^n\right)^2 = \left|\Gamma^{(n)}\right|^2 > 0, \\ b^n(\underline{x}) &= -2\,\underline{a}^n \cdot \underline{c}^n(x) = -2\left[a_1^n c_1^n(\underline{x}) + a_2^n c_2^n(\underline{x})\right], \\ c^n(\underline{x}) &= \underline{c}^n(x) \cdot \underline{c}^n(x) = \left(c_1^n(\underline{x})\right)^2 + \left(c_2^n(\underline{x})\right)^2 \geq 0. \end{aligned} \tag{A6}$$

By differentiating equation $(A4)$ and using relation $(A6)$, the partial derivatives of the Euclidean norm $r\left(\underline{x}, \underline{y}\right)$ of the vector $\underline{r}\left(\underline{x}, \underline{y}\right)$ are obtained as

$$\begin{aligned} \frac{\partial r\left(\underline{x}, \underline{y}(t)\right)}{\partial y_j} &= \frac{r\left(\underline{x}, \underline{y}(t)\right)}{r_j\left(\underline{x}, \underline{y}(t)\right)} \\ &= \frac{a_j^n\, t - c_j^n(\underline{x})}{\sqrt{a^n\, t^2 + b^n(\underline{x})\, t + c^n(\underline{x})}}, \quad j = 1, 2. \end{aligned} \tag{A7}$$

The components of the outward unit normal $\underline{\nu}\left(\underline{y}\right)$ at $\underline{y} \in \Gamma^{(n)}$ are given by

$$\begin{aligned} \nu_1\left(\underline{y}(t)\right) &= \frac{y_2^{(n)} - y_2^{(n-1)}}{\|\underline{y}^{(n)} - \underline{y}^{(n-1)}\|_2} = \frac{a_2^n}{\sqrt{a^n}}, \\ \nu_2\left(\underline{y}(t)\right) &= -\frac{y_1^{(n)} - y_1^{(n-1)}}{\|\underline{y}^{(n)} - \underline{y}^{(n-1)}\|_2} = -\frac{a_1^n}{\sqrt{a^n}}, \end{aligned} \tag{A8}$$

and hence the normal derivative of the function $r\left(\underline{x}, \underline{y}\right)$ along the boundary element $\Gamma^{(n)}$ can be expressed as

$$\begin{aligned} \frac{\partial r\left(\underline{x}, \underline{y}(t)\right)}{\partial \underline{\nu}\left(\underline{y}(t)\right)} &= \nabla_{\underline{y}} r\left(\underline{x}, \underline{y}(t)\right) \cdot \underline{\nu}\left(\underline{y}(t)\right) \\ &= \frac{a_1^n c_2^n(\underline{x}) - a_2^n c_1^n(\underline{x})}{\sqrt{a^n}} \frac{1}{\sqrt{a^n t^2 + b^n(\underline{x})\, t + c^n(\underline{x})}}. \end{aligned} \tag{A9}$$

If $E\left(\underline{x}, \underline{y}\right)$ is the fundamental solution for Helmholtz-type equations then its normal derivative along the boundary element $\Gamma^{(n)}$ is obtained by using the chain rule when differentiating $E\left(\underline{x}, \underline{y}\right)$ and is related to the normal derivative of the Euclidean norm $r\left(\underline{x}, \underline{y}\right)$ along the boundary element $\Gamma^{(n)}$, namely

$$\begin{aligned} \frac{\partial E\left(\underline{x}, \underline{y}(t)\right)}{\partial \underline{\nu}\left(\underline{y}(t)\right)} &= \nabla_{\underline{y}} E\left(\underline{x}, \underline{y}(t)\right) \cdot \underline{\nu}\left(\underline{y}(t)\right) \\ &= k\, E'\left[k\, r\left(\underline{x}, \underline{y}(t)\right)\right] \frac{\partial r\left(\underline{x}, \underline{y}(t)\right)}{\partial \underline{\nu}\left(\underline{y}(t)\right)}, \end{aligned} \tag{A10}$$

where $E'(z) = \dfrac{\mathrm{d}E(z)}{\mathrm{d}z}$ and $k > 0$. On using Eqs. $(A4)(A5)$, $(A9)$ and $(A10)$, the integration constants $A_n\left(\underline{x}\right)$ and $B_n\left(\underline{x}\right)$, $\underline{x} \in \overline{\Omega}$, defined by equation (17) can be expressed as

$$\begin{aligned} A_n\left(\underline{x}\right) &= k^2\left[a_1^n c_2^n(\underline{x}) - a_2^n c_1^n(\underline{x})\right] \\ &\quad \times \int_0^1 \frac{E'\left(k\sqrt{a^n\, t^2 + b^n(\underline{x})\, t + c^n(\underline{x})}\right)}{k\sqrt{a^n\, t^2 + b^n(\underline{x})\, t + c^n(\underline{x})}}\,\mathrm{d}t, \quad \underline{x} \in \overline{\Omega}, \end{aligned} \tag{A11}$$

$$B_n\left(\underline{x}\right) = \sqrt{a^n}\int_0^1 E\left(k\sqrt{a^n\, t^2 + b^n(\underline{x})\, t + c^n(\underline{x})}\right)\mathrm{d}t, \quad \underline{x} \in \overline{\Omega}. \tag{A12}$$

When calculating the integration constants $A_n\left(\underline{x}\right)$ and $B_n\left(\underline{x}\right)$, two situations can appear depending on whether or not the collocation point $\underline{x}$ belongs to the element $\Gamma^{(n)}$ over

which the integration is performed. The first situation involves singular integrands and in this case, the integration is performed in the sense of the Cauchy principal value, whilst the second one admits a standard quadrature formula. In this paper, the Trapezoidal Rule of order $N_q = 100$ has been performed for calculating the non-singular integrals. It should be mentioned that a standard Gaussian quadrature could also be employed, provided that the parametrisation of the boundary element $\Gamma^{(n)}$ is made with respect to $t \in [-1, 1]$, see Chen and Zhou [34].

A.2 Helmholtz equation

In the case of the Helmholtz equation, the fundamental solution and its normal derivative along the boundary element $\Gamma^{(n)}$ are given by

$$E_{\mathrm{H}}\left(\underline{x}, \underline{y}(t)\right) = \frac{\mathrm{i}}{4} H_0^{(1)}\left[k\, r\left(\underline{x}, \underline{y}(t)\right)\right],$$
$$\frac{\partial E_{\mathrm{H}}\left(\underline{x}, \underline{y}(t)\right)}{\partial \underline{\nu}\left(\underline{y}(t)\right)} = \frac{\mathrm{i}k}{4}\, \mathrm{e}^{\pi \mathrm{i}}\, H_1^{(1)}\left[k\, r\left(\underline{x}, \underline{y}(t)\right)\right] \frac{\partial r\left(\underline{x}, \underline{y}(t)\right)}{\partial \underline{\nu}\left(\underline{y}(t)\right)}, \tag{A13}$$

where $H_0^{(1)}$ and $H_1^{(1)}$ are the modified Hankel functions of the first kind of order zero and one, respectively, and the following relation has been used $H_0^{(1)'}(z) = \mathrm{e}^{\pi \mathrm{i}} H_1^{(1)}(z)$ for $z \in \mathbb{C}$, see Abramowitz and Stegun [45]. Hence the integration constants $A_n\left(\underline{x}\right)$ and $B_n\left(\underline{x}\right)$, $\underline{x} \in \overline{\Omega}$, are given by

$$A_n\left(\underline{x}\right) = \frac{\mathrm{i}k^2}{4}\, \mathrm{e}^{\pi \mathrm{i}} \left[a_1^n c_2^n(\underline{x}) - a_2^n c_1^n(\underline{x})\right] \times \int_0^1 \frac{H_1^{(1)}\left(k\sqrt{a^n\, t^2 + b^n(\underline{x})\, t + c^n(\underline{x})}\right)}{k\sqrt{a^n\, t^2 + b^n(\underline{x})\, t + c^n(\underline{x})}}\, \mathrm{d}t, \tag{A14}$$

$$B_n\left(\underline{x}\right) = \frac{\mathrm{i}\sqrt{a^n}}{4} \int_0^1 H_0^{(1)}\left(k\sqrt{a^n\, t^2 + b^n(\underline{x})\, t + c^n(\underline{x})}\right) \mathrm{d}t. \tag{A15}$$

Case 1. $\underline{x} \notin \Gamma^{(n)}$ i.e., $\underline{x} = \underline{x}^{(m)}, m \neq n$)

$$A_n\left(\underline{x}\right) \approx \frac{\mathrm{i}k^2}{4}\, \mathrm{e}^{\pi \mathrm{i}} \left[a_1^n c_2^n(\underline{x}) - a_2^n c_1^n(\underline{x})\right] \frac{1}{N_q} \times \left(\frac{1}{2} \frac{H_1^{(1)}(k\, r_0)}{k\, r_0} + \sum_{j=1}^{N_q - 1} \frac{H_1^{(1)}\left(k\, r_j\right)}{k\, r_j} + \frac{1}{2} \frac{H_1^{(1)}\left(k\, r_{N_q}\right)}{k\, r_{N_q}}\right), \tag{A16}$$

$$B_n\left(\underline{x}\right) \approx \frac{\mathrm{i}\sqrt{a^n}}{4} \frac{1}{N_q} \times \left(\frac{1}{2} H_0^{(1)}(k\, r_0) + \sum_{j=0}^{N_q - 1} H_0^{(1)}\left(k\, r_j\right) + \frac{1}{2} H_0^{(1)}\left(k\, r_{N_q}\right)\right), \tag{A17}$$

where

$$r_j = \sqrt{a^n \frac{j^2}{N_q^2} + b^n(\underline{x}) \frac{j}{N_q} + c^n(\underline{x})}, \quad j = 0, \ldots, N_q. \tag{A18}$$

Case 2. $\underline{x} \in \Gamma^{(n)}$ i.e., $\underline{x} = \underline{x}^{(n)}$)

In this case $\underline{c}^n(\underline{x}^{(n)}) = \underline{a}^n/2$, $a_1^n c_2^n(\underline{x}^{(n)}) - a_2^n c_1^n(\underline{x}^{(n)}) = 0$ and $4c^n(\underline{x}^{(n)}) = -b^n(\underline{x}^{(n)}) = a^n$, which implies

$$A_n\left(\underline{x}^{(n)}\right) = 0, \quad B_n\left(\underline{x}^{(n)}\right) = \frac{\mathrm{i}}{2k} \int_0^{k\sqrt{a^n}/2} H_0^{(1)}(t)\, \mathrm{d}t. \tag{A19}$$

The integral in equation (*A*19) is calculated using the following exact formula, see Abramowitz and Stegun [45],

$$\int_0^z H_0^{(1)}(\zeta)\mathrm{d}\zeta = z\left\{H_0^{(1)}(z) + \frac{\pi}{2}\left[-\mathbb{H}_1(z) H_0^{(1)}(z) + \mathbb{H}_0(z) H_1^{(1)}(z)\right]\right\}, \quad z \in \mathbb{C}, \tag{A20}$$

where the Struve functions of order zero, $\mathbb{H}_0$, and one, $\mathbb{H}_1$, are given by

$$\mathbb{H}_0(z) = \frac{2}{\pi} \sum_{m=0}^{\infty} (-1)^m \frac{z^{2m+1}}{\prod_{j=0}^{m} (2j+1)^2},$$
$$\mathbb{H}_1(z) = \frac{2}{\pi} \sum_{m=0}^{\infty} (-1)^m \frac{z^{2m+2}}{(2m+3) \prod_{j=0}^{m} (2j+1)^2}, \quad z \in \mathbb{C}. \tag{A21}$$

A.3 Modified helmholtz equation

In the case of the modified Helmholtz equation, the fundamental solution and its normal derivative along the boundary element $\Gamma^{(n)}$ are given by

$$E_{\mathrm{MH}}\left(\underline{x}, \underline{y}(t)\right) = \frac{1}{2\pi} K_0\left[k\, r\left(\underline{x}, \underline{y}(t)\right)\right],$$
$$\frac{\partial E_{\mathrm{MH}}\left(\underline{x}, \underline{y}(t)\right)}{\partial \underline{\nu}\left(\underline{y}(t)\right)} = -\frac{k}{2\pi} K_1\left[k\, r\left(\underline{x}, \underline{y}(t)\right)\right] \frac{\partial r\left(\underline{x}, \underline{y}(t)\right)}{\partial \underline{\nu}\left(\underline{y}(t)\right)}, \tag{A22}$$

where K_0 and K_1 are the modified Bessel functions of the second kind of order zero and one, respectively, and the following relation has been used $K_0'(z) = -K_1(z)$ for $z \in \mathbb{C}$, see Abramowitz and Stegun [45]. Hence the integration constants $A_n\left(\underline{x}\right)$ and $B_n\left(\underline{x}\right)$, $\underline{x} \in \overline{\Omega}$, are given by

$$A_n\left(\underline{x}\right) = -\frac{k^2}{2\pi}\left[a_1^n c_2^n(\underline{x}) - a_2^n c_1^n(\underline{x})\right] \times \int_0^1 \frac{K_1\left(k\sqrt{a^n\, t^2 + b^n(\underline{x})\, t + c^n(\underline{x})}\right)}{k\sqrt{a^n\, t^2 + b^n(\underline{x})\, t + c^n(\underline{x})}}\, \mathrm{d}t, \tag{A23}$$

$$B_n\left(\underline{x}\right) = \frac{\sqrt{a^n}}{2\pi}\int_0^1 K_0\left(k\sqrt{a^n\, t^2 + b^n(\underline{x})\, t + c^n(\underline{x})}\right)\, \mathrm{d}t. \tag{A24}$$

Case 1. $\underline{x} \notin \Gamma^{(n)}$ i.e. $\underline{x} = \underline{x}^{(m)}$, $m \neq n$)

$$A_n\left(\underline{x}\right) \approx -\frac{k^2}{2\pi}\left[a_1^n c_2^n(\underline{x}) - a_2^n c_1^n(\underline{x})\right]\frac{1}{N_q} \times \left(\frac{1}{2}\frac{K_1\left(k\, r_0\right)}{k\, r_0} + \sum_{j=1}^{N_q-1}\frac{K_1\left(k\, r_j\right)}{k\, r_j} + \frac{1}{2}\frac{K_1\left(k\, r_{N_q}\right)}{k\, r_{N_q}}\right), \tag{A25}$$

$$B_n\left(\underline{x}\right) \approx \frac{\sqrt{a^n}}{2\pi}\frac{1}{N_q} \times \left(\frac{1}{2}K_0\left(k\, r_0\right) + \sum_{j=0}^{N_q-1} K_0\left(k\, r_j\right) + \frac{1}{2}K_0\left(k\, r_{N_q}\right)\right). \tag{A26}$$

Case 2. $\underline{x} \in \Gamma^{(n)}$ i.e. $\underline{x} = \underline{x}^{(n)}$)

In this case $\underline{c}^n(\underline{x}^{(n)}) = \underline{a}^n/2$, $a_1^n c_2^n(\underline{x}^{(n)}) - a_2^n c_1^n(\underline{x}^{(n)}) = 0$ and $4c^n(\underline{x}^{(n)}) = -b^n(\underline{x}^{(n)}) = a^n$, which implies

$$A_n\left(\underline{x}^{(n)}\right) = 0, \quad B_n\left(\underline{x}^{(n)}\right) = \frac{1}{k\,\pi}\int_0^{k\sqrt{a^n}/2} K_0(t)\, \mathrm{d}t. \tag{A27}$$

The integral in equation $(A27)$ is calculated using the following exact formula, see Abramowitz and Stegun [45],

$$\int_0^x K_0(t)\mathrm{d}t = x\left\{K_0(x) + \frac{\pi}{2}\left[\mathbb{L}_1(x)K_0(x) + \mathbb{L}_0(x)K_1(x)\right]\right\}, \quad x > 0, \tag{A28}$$

where the modified Struve functions of order zero, $\mathbb{L}_0$, and one, $\mathbb{L}_1$, are given by

$$\mathbb{L}_0(z) = -\mathrm{i}\mathbb{H}_0(\mathrm{i}z) = \frac{2}{\pi}\sum_{m=0}^{\infty}\frac{z^{2m+1}}{\prod_{j=0}^{m}(2j+1)^2},$$

$$\mathbb{L}_1(z) = -\mathbb{H}_1(\mathrm{i}z) = \frac{2}{\pi}\sum_{m=0}^{\infty}\frac{z^{2m+2}}{(2m+3)\prod_{j=0}^{m}(2j+1)^2}, \quad z \in \mathbb{C}. \tag{A29}$$

A.4 Nag subroutines

The values of the modified Bessel functions of the second kind of order zero, K_0, and one, K_1, and the Hankel functions of the first kind of order zero, $H_0^{(1)}$, and one, $H_1^{(1)}$, for $t > 0$ have been calculated using the following NAG subroutines S18ACF (K_0), S18ADF (K_1) and S17DLF ($H_0^{(1)}$ and $H_1^{(1)}$), see [46]. The values of the Struve and modified Struve functions $\mathbb{H}_j$ and $\mathbb{L}_j$, $j = 0, 1$, occurring in Eqs. $(A20)$ and $(A28)$, respectively, have been calculated by considering N_t terms in formulae $(A21)$ and $(A29)$, with the mention that $N_t = 500$ was found to be sufficiently large that a further increase in this value does not affect significantly the accuracy of the numerical results.

Acknowledgements The author would like to thank Dr. Lionel Elliott from the Department of Applied Mathematics at the University of Leeds for all his encouragement in performing this research work. The suggestions made by the referees are also gratefully acknowledged.

References

1. Kubo S (1988) Inverse problems related to the mechanics and fracture of solids and structures. JSME Int J 31:157–166.
2. Hadamard J (1923) Lectures on Cauchy problem in linear partial differential equations. Oxford University Press, London
3. Wei X, Chandra A, Leu L-J, Mukherjee S (1994) Shape optimization in elasticity and elasto-viscoplasticity by the boundary element method. Int J Solids Struct 31:533–550
4. Shi X, Mukherjee S (1999) Shape optimization in the three-dimensional linear elasticity by the boundary contour method. Engng Anal Boundary Elements 23:627–637
5. Bobaru F, Mukherjee S (2001) Shape sensitivity analysis and shape optimization in planar elasticity using the element-free Galerkin method. Comput Meth Appl Mech Engng 190:4319–4337.
6. Calvo E, Garcia L (2001) Shape design sensitivity analysis in elasticity using the boundary element method. Engng Anal Boundary Elements 25:887–896
7. Tafreshi A (2002) Shape design sensitivity analysis in 2D anisotropic structures using the boundary element method. Engng Anal Boundary Elements 26:237–251
8. Ikehata M (1998) Size estimation of inclusion. J Inverse Ill-Posed Probl 6:127–140
9. Tanaka M, Yamagiwa K (1989) A boundary element for some inverse problems in elastodynamics. Appl Math Modelling 13:307–312

10. Bezerra LM, Saigal S (1993) A boundary element formulation for the inverse elastostatics problem (IESP) of flaw detection. Int J Numer Meth Engng 36:2189–2202
11. Kassab AJ, Moslehy FA, Daryapurkar AB (1994) Nondestructive detection of cavities by an inverse elastostatics boundary element method. Engng Anal Boundary Elements 13:45–55
12. Mellings SC, Aliabadi MH (1995) Flaw identification using the boundary element method. Int J Numer Meth Engng 38:399–419
13. Ulrich TW, Moslehy FA, Kassab AJ (1996) A BEM based pattern search solution for a class of inverse elastostatic problems. Int J Solids Struct 33:2123–2131
14. Marin L, Elliott L, Ingham DB, Lesnic D (2003) Identification of material properties and cavities in two-dimensional linear elasticity. Comput Mech 31:293–300
15. Aparicio ND, Pidcock MK (1996) The boundary inverse problem for the Laplace equation in two dimensions. Inverse Problems 12:565–577
16. Beretta E, Vessela S (1998) Stable determination of boundaries from Cauchy data. SIAM J Math Anal 30:220–232
17. Bukhgeim AL, Cheng J, Yamamoto M (1999) Stability for an inverse problem of determining a part of the boundary. Inverse Problems 15:1021–1032
18. Hsieh CK, Kassab AJ (1986) A general method for the solution of inverse heat conduction problems with partially unknown system geometries. Int J Heat Mass Transfer 29:47–58
19. Huang CC, Chao BH (1997) An inverse geometry problem for identifying irregular boundary configurations. Int J Heat Mass Transfer 40:2045–2053
20. Huang CC, Tsai CC (1998) A transient inverse two-dimensional geometry problem in estimating time-dependent irregular boundary configurations. Int J Heat Mass Transfer 41:1707–1718
21. Hon YC, Zongmin W (2000) A numerical computation for inverse boundary determination problem. Engng Anal Boundary Elements 24:599–606
22. Park HM, Ku JH (2001) Shape identification for natural convection problems. Commun Numer Meth Engng 17:871–880
23. Lesnic D, Berger JR, Martin PA (2002) A boundary element regularization method for the boundary determination in potential corrosion damage. Inverse Probl Engng 10:163–182
24. Marin L, Lesnic D (2003) BEM first-order regularisation method in linear elasticity for boundary identification. Comput Meth Appl Mech Engng 192:2059–2071
25. Beskos DE (1997) Boundary element method in dynamic analysis: Part II (1986–1996). ASME Appl Mech Rev 50:149–197
26. Chen JT, Wong FC (1998) Dual formulation of multiple reciprocity method for the acoustic mode of a cavity with a thin partition. J Sound Vibration 217:75–95
27. Harari I, Barbone PE, Slavutin M, Shalom R (1998) Boundary infinite elements for the Helmholtz equation in exterior domains. Int J Numer Meth Engng 41:1105–1131
28. Hall WS, Mao XQ (1995) A boundary element investigation of irregular frequencies in electromagnetic scattering. Engng Anal Boundary Elements 16:245–252
29. Kraus AD, Aziz A, Welty J (2001) Extended surface heat transfer. John Wiley & Sons, New York
30. Hansen PC (1992) Analysis of discrete and ill-posed problems by means of the L-curve. SIAM Rev 34:561–580
31. Morozov VA (1966) On the solution of functional equations by the method of regularization. Soviet Math Dokl 7:414–417
32. Wahba G (1977) Practical approximate solution to linear operator equations when the data is noisy. SIAM J Numer Anal 14:651–667
33. Kellogg OD (1923) Foundations of potential theory. New Haven, Dover
34. Chen G, Zhou J (1992) Boundary element methods. Academic Press, London
35. Marin L, Elliott L, Heggs PJ, Ingham DB, Lesnic D, Wen X (2003) An alternating iterative algorithm for the Cauchy problem associated to the Helmholtz equation. Comput Meth Appl Mech Engng 192:709–722
36. Marin L, Elliott L, Heggs PJ, Ingham DB, Lesnic D, Wen X (2003) Conjugate gradient-boundary element solution to the Cauchy problem for Helmholtz-type equations. Comput Mech 31:367–377
37. Gill PE, Murray W, Wright MH (1981) Practical optimization. Academic Press, London
38. Peneau S, Jarny Y, and Sarda A (1994) Isotherm shape identification for a two-dimensional heat conduction problem. In: Bui HD, Tanaka M, Bonnet M, Maigre H, Luzzato E, Reynier M (eds), Inverse Problems in Engineering Mechanics, pp. 47–53. Balkema, Rotterdam
39. Birginie J-M, Allard F, Kassab AJ (1996) Application of trigonometric boundary elements to heat and mass transfer problems. In: Brebbia CA, Martin JB, Aliabadi MH, Haie N (eds), BEM 18, pp. 65–74. Braga, Portugal
40. Tikhonov AN, Leonov AS, Yagola AG (1998) Nonlinear Ill-Posed Problems. Chapman & Hall, London
41. Hansen PC (2001) The L-curve and its use in the numerical treatment of inverse problems. In: Johnston P (ed), Computational Inverse Problems in Electrocardiology, pp. 119–142. WIT Press, Southampton
42. Hanke M (1996) Limitations of the L-curve method in ill-posed problems. BIT 36:287–301
43. Vogel CR (1996) Non-convergence of the L-curve regularization parameter method. Inverse Probl 12:535–547
44. Hansen PC (1993) The use of the L-curve in the regularization of discrete ill-posed problems. SIAM J Sci Comput 14:1487–1503
45. Abramowitz M, Stegun JA (1965) Handbook of mathematical functions. Dover Publications, New York
46. NAG Fortran Library Manual, Mark 20. The Numerical Algorithms Group Limited, 2001